The Image Fusion Technique for Cochlear Implant Imaging: A Study of its Application for Different Electrode Arrays

Sini Sipari, Matti Iso-Mustajärvi, Mervi Könönen, Heikki Löppönen, and Aarno Dietz

Department of Otorhinolaryngology, Kuopio University Hospital, Kuopio, Finland

Objectives: To investigate the benefits of the image fusion technique for precise postoperative assessment of intracochlear placement with six different electrode arrays.
Study Design: Consecutive retrospective case study.
Settings: Tertiary referral center.
Patients: Analyses of imaging data of 30 patients implanted with six different electrode arrays.
Interventions: Electrode reconstructions obtained from postoperative cone-beam computed tomography (CBCT) were overlaid onto preoperative magnetic resonance imaging (MRI) and/or high-resolution computed tomography (HRCT) registrations to create artefact-free images.
Main Outcome Measures: Each electrode's intracochlear position was analyzed with the image fusion reconstructions and compared with the results obtained by CBCT alone. The electrode location was classified according to its position in relation to the basal membrane at four different insertion angles.
Results: In 40 out of 151 measurements (26.5%), the location grading obtained by CBCT alone changed after the assessment with the image fusion reconstructions. A significant association was found between deep insertions (over 360 degrees) and the effectiveness of image fusion ($p = 0.019$). The difference between the impact of the fusion technique for the basal turn versus the apical part was highly significant ($p = 0.001$). There was no significant difference between the effectiveness of the image fusion and the different electrodes.
Conclusions: By utilizing an image fusion technique, a more accurate assessment of electrode placement could be achieved for all types of electrodes. Image fusion was especially beneficial for insertions beyond 360 degrees.
Key Words: Array—Cone-beam computed tomography—Computed tomography—Electrode—Electrode location—Image fusion—Imaging—Insertion trauma—Magnetic resonance imaging.

Otol Neurotol **41:**e216–e222, 2020.

The electrode location within the inner ear has been shown to significantly contribute to hearing outcomes achieved with cochlear implants (1–5). Electrode placement into the scala tympani is recommended as this has been associated with superior hearing outcomes (5). Electrode translocation and insertion into the scala vestibuli carry a greater risk for damaging the delicate intracochlear neural structures thus compromising the postoperative hearing performance (2,3,5).

Postoperative radiological evaluation after cochlear implantation is beneficial for the assessment of insertion trauma, quality control, and documentation. It may also help in the individual programming of the sound processor. Accurate postoperative imaging is needed for identifying possible electrode tip folding, migration, bulging and scala translocation (6,7). It is also indispensable for the evaluation of new electrode arrays and for the development of surgical techniques.

Magnetic resonance imaging (MRI) and high-resolution computed tomography (HRCT) are used for pre-implant evaluation to rule out cochlear malformation and retrocochlear pathology (7,8). More recently, cone-beam computed tomography (CBCT) has emerged as the modality of choice for postoperative imaging of cochlear implants. The advantages of CBCT are 1) significantly reduced radiation exposure and 2) considerably smaller electrode artefacts as compared with spiral HRCT (9–12). However, metallic artefacts still impair the overall image quality, which often limits the accurate assessment of the position of the electrode in the basal turn (13–15).

Several studies have shown that the accuracy can be improved by the image fusion technique (16–20). 3D models of the array images are created from the postoperative CBCT scans by HU (Hounsfield Units) thresholding and then overlaid onto the preoperative MRI and/or CT registrations. This technique significantly improves the image quality by eliminating the artefacts, and allows for a reliable and accurate evaluation of the location of the electrode. The technique has been validated against histology and proved to be a valid method for trauma assessment (20).

Address correspondence and reprint requests to Sini Sipari, M.D., Department of Otorhinolaryngology, Kuopio University Hospital, P.O. Box 100, 70029 Kuopio, Finland; E-mail: sini.sipari@kuh.fi
The authors disclose no conflicts of interest.
DOI: 10.1097/MAO.0000000000002479

As preoperative imaging with MRI and computed tomography (CT), in conjunction with postoperative evaluation with CBCT, has become the standard protocol for cochlear implantation in an increasing number of institutions, it is appropriate to assess the possible benefits of image fusion of these imaging modalities.

The aim of the study is to evaluate the clinical application of image fusion technique for the assessment of electrode location for six different commercially available electrode arrays in comparison with the results obtained by CBCT alone.

MATERIAL AND METHODS

This retrospective study was conducted in the Department of Otorhinolaryngology of the Kuopio University Hospital. The study received institutional approval. A total of 30 patients implanted between November 17, 2015 and February 27, 2019 were selected from the CI database on the basis of a specific implanted CI device. We selected five consecutively implanted patients for whom we had the relevant imaging data available for each of the six different electrode arrays (Table 1). Data were obtained from the medical records, including pre- and postoperative imaging data. Postoperative CBCT was re-evaluated by the authors (S.S., M.I., A.D.) for insertion trauma and electrode location. Image fusions were reconstructed from the preoperative MRI and CT scans and the postoperative CBCT scans.

Electrodes

The following electrode arrays were used:

Med-El Flex28 (Med-El GmbH, Innsbruck, Austria).
A straight electrode with an insertion length of 28 mm with eight basal full-band (two 0.8 mm × 0.5 mm contacts on each side) and four apical half-band electrode contacts (0.8 mm × 0.5 mm on one side) spaced over a 23.1 mm stimulation range. The diameter at the apical end is 0.5 × 0.4 mm and 0.8 mm at the basal end.
HiFocus Mid-Scala electrode (Advanced Bionics, Valencia, CA)
A precurved electrode with a total length of 23.7 mm and an insertion length of 18.5 mm with 16 half-band electrode contacts (0.4 mm × 0.4 mm). The diameter is 0.76 mm at the basal part and 0.52 mm at the tip.
HiFocus SlimJ (Advanced Bionics, Valencia, CA)
A slim lateral wall electrode curved at the tip with an insertion length of 23 mm and 16 electrode contacts (0.47 × 0.36 mm). The dimensions at the apical and basal part are 0.55 × 0.26 mm and 0.76 × 0.56 mm, respectively.

TABLE 1. *Demographics of the patients*

Patient	Electrode	Side	Approach	Etiology	Gender	Age at Implantation	IDA (degrees)
1	Flex28	dx	RW	Sudden SNHL	F	56	610
2	Flex28	sin	RW	Progressive SNHL	M	82	485
3	Flex28	sin	RW	Sudden SNHL	M	25	480
4	Flex28	sin	RW	Congenital SNHL	F	42	635
5	Flex28	dx	RW	KID syndrome	F	39	485
6	Mid-Scala	sin	RW	Meningitis	M	67	360
7	Mid-Scala	dx	RW	Progressive SNHL	F	52	345
8	Mid-Scala	dx	ERW	MELAS	F	57	360
9	Mid-Scala	dx	ERW	Progressive SNHL	F	33	345
10	Mid-Scala	sin	C, ST	Progressive SNHL (DM1)	M	64	360
11	CI532	sin	RW	Congenital SNHL	M	45	400
12	CI532	dx	RW	Congenital SNHL	F	45	390
13	CI532	dx	RW	Premature birth	M	24	380
14	CI532	sin	RW	Progressive SNHL	F	63	390
15	CI532	dx	RW	Progressive SNHL	F	66	380
16	SlimJ	dx	RW	KID, connexin26	M	41	380
17	SlimJ	dx	RW	Progressive SNHL	F	68	390
18	SlimJ	sin	RW	Progressive SNHL	M	65	360
19	SlimJ	dx	RW	Progressive SNHL	M	86	360
20	SlimJ	sin	C, SV	Otosclerosis	M	40	420
21	CI522	sin	RW	Congenital SNHL	M	13	450
22	CI522	sin	C, ST	Congenital SNHL	M	11	420
23	CI522	dx	RW	Congenital SNHL	M	20	440
24	CI522	dx	RW	Menière	F	59	400
25	CI522	sin	RW	Progressive SNHL	F	62	470
26	EVO	dx	RW	Progressive SNHL	M	81	450
27	EVO	sin	ERW	Progressive SNHL	F	80	450
28	EVO	dx	RW	Menière	F	75	360
29	EVO	sin	RW	Sudden SNHL	F	88	460
30	EVO	dx	ERW	Menière	F	71	450

C indicates cochleostomy; DM1, diabetes mellitus type 1; ERW, extended round window; F, female; IDA, insertion depth angle; M, male; RW, round window; SNHL, sensorineural hearing loss; ST, scala tympani; SV, scala vestibuli.

Slim Modiolar CI532 (Cochlear, Sydney, Australia)
A perimodiolar electrode with 22 half-band electrode contacts of $0.2 \times 0.37–0.4 \times 0.4–0.5$ mm and an insertion length of 17 mm. The apical diameter is 0.35×0.4 mm and the basal diameter 0.475×0.5 mm.
Slim Straight CI522 (Cochlear, Sydney, Australia)
This is a lateral wall electrode with 22 half-band electrode contacts of $0.2 \times 0.35–0.6 \times 0.35–0.4$ mm. The electrode's active length is 20 mm and the insertion depth can be adjusted from 20 to 25 mm.
Oticon Evo (Oticon Medical, Copenhagen, Denmark)
A slim straight lateral wall electrode with 20 full-band electrode contacts along the active length of 24 mm with a maximum insertion length of 25 mm. The 10 basal electrode contacts are $0.475 \text{ mm} \times 0.5$ mm and the apical 10 contacts are $0.475 \text{ mm} \times 0.4$ mm. The basal and apical diameters are 0.5 mm and 0.4 mm, respectively.

Imaging

According to our clinical protocol, the preoperative evaluation for patients undergoing cochlear implantation includes MRI and HRCT scanning, usually performed at the referring clinic. For the HRCT, the following variations in the protocol were applied: 128×0.6 mm collimation, 0.8 pitch, qualityref mAs 210 @120 kV, CTDIvol 30.30 mGy. MR imaging was performed with a 1.5T scanner (Siemens AvantoFit, Erlangen, Germany). The T2-weighted 3D Constructive Interference in Steady State (CISS) sequence with isotropic voxels (resolution 0.6 mm, repetition time 1200 ms, echo time 262 ms, flip angle 150 degrees) was scanned, and images were reconstructed to a resolution of $0.3 \text{ mm} \times 0.3$ mm. The CISS-sequence provides a strong contrast between cerebrospinal fluid and other structures, allowing the detection of cochlear fibrosis and obliteration (21–23). Further, the liquid-filled cochlear turns, and in numerous cases even the basilar membrane (BM), can be visualized (19). Therefore, the CISS sequence was used for the image fusions for the optimal visualization of the scalae and the BM. Postoperative CBCT imaging was arranged on the first postoperative day to evaluate electrode localization and insertion trauma. Scanning was performed with ProMax 3D Max (Planmeca Oy, Helsinki, Finland) with the following protocol: volume 50×55 mm, 96 kV, 5 to 7.1 mA, 15 seconds, dose-area product 7.06 to 8.99 dgycm^2, and voxel size 150 μm. Application of metallic artefact reduction was run on the default mode ''midi.''

Image Fusion

Image fusion reconstructions of the pre- and postoperative scans were fused with automatic image fusion software BrainLab (iPlan Net 3.6.0 Build 77, BrainLab AG, Munich, Germany). 3D models of the electrodes were created from the post-insertion CBCTs using HU thresholding. The models were overlaid onto the preoperative MRI and CT registrations to create images with more accurate electrode locations. An axis parallel to the modiolus running from the cochlear base to the apex was created; two perpendicular cross-sections and the cochlea projection were reconstructed.

The available image slice thickness for the fusion process was 1 mm for HRCT, and 0.6 mm for MRI respectively. The raw data is usually kept for a short time after imaging, and slices commonly used for radiological assessment are stored for later evaluation. Therefore, the raw data was not available for the reconstructions.

Radiologic Assessment of Electrode Location

The electrode locations were determined at insertion depth angles (IDA) of 90, 180, 270, 360 degrees and additionally at 450, 540 degrees, and at the tip electrode when necessary. The electrode location grading of the postoperative CBCT and the fusion imaging was accomplished by visual assessment based on a scalar division described by Sipari et al. (19).

According to the electrode's position, its placement was classified into four categories: scala tympani (ST); scala vestibuli (SV); indifferent (I) corresponding with elevation or rupture of the BM; not able to be determined (N/D) whenever the electrode location could not be pinpointed (Table 2). We compared the results obtained by the fusion images with those of CBCT alone. These results were then analyzed with respect to whether the fusion technique had facilitated the evaluation of electrode placement or even changed the location classification. The evaluation was made with postoperative CBCT and both the preoperative MRI and HRCT image fusion reconstructions. The results were compared and the image modalities were analyzed with respect to whether the fusion images had improved the evaluation or even changed the location grading. The impact of image fusion on the location grading was classified into three categories: 1) significant impact, changing location grading when compared with CBCT alone, 2) minor impact on location grading, making the assessment more accurate and reliable (the grading did not change in these cases), 3) no impact on location grading, with no additional benefit over CBCT (Table 2).

Statistical Analysis

Data are shown as means with standard deviations or frequencies with percentages. Continuous variables were compared by independent samples t test and categorical variables Fisher's exact test. Presence of ''image fusion change the location grading'' between IDAs of 90, 180, 270, 360 degrees and additionally with 450, 540 degrees, and the tip of the electrode, were compared by χ^2 test and Cochran's Q paired samples tests. Statistical analyses were executed with SPSS software (IBM SPSS Statistics for Windows, Version 22.0. Armonk, NY: IBM Corp). P-values < 0.05 were considered statistically significant.

RESULTS

The electrode location was assessed in both MRI and CT fusions. In the majority of cases, MRI allowed for a more precise evaluation than CT. In two cases, however, the CT images described the electrode location in more detail.

In 13 out of 30 cases (40.3%), fusion image reconstruction had a significant impact on location grading. In 12 of these cases, the grading changed from ''not able to be determined'' to a defined grade and in one case ''BM elevation or rupture'' changed to translocation. A minor impact was found in two cases in which the fusion reconstructions aided in the definite grading (Table 2). Altogether, the fusion technique was found to have been helpful and improved location grading in every second case.

In 26.5% of all the 151 measurement points, the grading changed, i.e., the image fusion exerted a significant impact on the evaluation. When the grading was

TABLE 2. *Electrode location in the scalae at different IDAs on CBCT and image fusion*

Patient	Electrode	IDA degrees	90 degrees CBCT	90 degrees Fusion	180 degrees CBCT	180 degrees Fusion	270 degrees CBCT	270 degrees Fusion	360 degrees CBCT	360 degrees Fusion	Tip CBCT	Tip Fusion
1	Flex28	610	ST	ST	ST	ST	ND	ST	ND	ST	ND	ST
2	Flex28	485	ST	ST	ST	ST	ST	ST	ST	ST	ST	ST
3	Flex28	480	ST	ST	ST	ST	ST	ST	ST	ST	ST	ST
4	Flex28	635	ST	ST	ND	ST	ST	ST	ND	I	ND	I
5	Flex28	485	ST	ST	ST	ST	ST	ST	ND	ST	ND	ST
6	Mid-Scala	360	ST	ST	ST	ST	ST	ST	ST	ST		
7	Mid-Scala	345	ST	ST	ST	ST	ST	ST	ST	ST		
8	Mid-Scala	360	ST	ST	ST	ST	ST	ST	ST	ST		
9	Mid-Scala	345	ST	ST	ST	ST	ST	ST	ST	ST		
10	Mid-Scala	360	ST	ST	ND	ST	ST	ST	ST	ST		
11	CI532	400	ST	ST	ST	ST	ST	ST	ST	ST	ST	ST
12	CI532	390	ST	ST	ST	ST	ST	ST	ND	ST	ND	ST
13	CI532	380	ST	ST	ST	ST	ST	ST	ST	ST		
14	CI532	390	ND	ST	ND	ST	ND	ST	ND	ST	ND	ST
15	CI532	380	ND	ST	ND	ST	ND	I	ND	ST		
16	SlimJ	380	ST	ST	ST	ST	ST	ST	ST	ST		
17	SlimJ	390	ST	ST	ST	ST	ST	ST	ST	ST	ST	ST
18	SlimJ	360	ST	ST	ST	ST	ST	ST	ST	ST		
19	SlimJ	360	ST	ST	ST	ST	ST	ST	ND	ST		
20	SlimJ	420	ND	SV	ND	SV	ND	SV	ND	SV	ND	SV
21	CI522	450	ND	ST	ST	ST	ST	ST	ST	ST	ND	ST
22	CI522	420	ST	ST	ST	ST	ST	ST	ST	ST	ST	ST
23	CI522	440	ST	ST	ST	ST	ST	ST	ST	ST	ST	ST
24	CI522	400	ST	ST	ST	ST	ST	ST	ST	ST	ST	ST
25	CI522	470	ST	ST	I	I	ST	ST	ST	ST	ND	I
26	EVO	450	SV	SV	ST	ST	ST	ST	ST	ST	ST	ST
27	EVO	450	ST	ST	I	SV	I	I	ND	SV	SV	SV
28	EVO	360	ST	ST	ST	ST	ST	ST	ST	ST		
29	EVO	460	ST	ST	ST	ST	ST	ST	ST	ST	ST	ST
30	EVO	450	ST	ST	ST	ST	ST	ST	ND	I	ND	ST

Location defined as I, indifferent corresponding with elevation or rupture of the BM. ND, not determinable; ST, scala tympani; SV, scala vestibule.

The impact of image fusion for the location assessment classified into three categories: light gray: image fusion changed the location grading, dark grey: image fusion made the assessment more accurate and reliable, white: image fusion gave no additional benefit to the assessment. CBCT indicates cone-beam computed tomography; IDA, insertion depth angle.

examined with respect to each separate IDA, the incidence of there being a significant impact of image fusion was as follows: 90 degrees: 13.3%, 180 degrees: 20%, 270 degrees: 13.3%, 360 degrees: 33.3%, 450 degrees: 54.5%, 540 degrees: 100%. A significant association was found between the growing IDA and the impact of image fusion (Cochran's Q paired samples tests; $p = 0.019$).

When splitting the cohort of measurement points into those with an IDA less than or equal to 360 degrees and IDA more than 360 degrees, location grading changed in 20 and 51.6%, respectively. The difference between the impact in the basal turn and the deeper IDAs was found to be highly significant (χ^2 test; $p = 0.001$).

The artefacts of each type of array were found to be diverse, with some arrays generating more artefact than the others. The CI532 and EVO created the largest, mostly continuous artefacts through the linear length. Mid-scala had the least artefact, with symmetrical round shapes, yet one array in the group displayed large asymmetrical artefacts for some unknown reason. Flex28, SlimJ, and CI522 were placed in between with some artefacts, i.e., some lining up and artefact tails were observed. The typical features of each type are described in Figure 1. The artefacts were considered to be extensive if they were asymmetrical, large in relation to the electrode size, if they had rays or arches blurring the surroundings structures or when they were lining up as a continuous artefact along the array. The artefacts were visually assessed, not measured, since we considered it sufficient for our objective to determine whether image fusion had been advantageous in location assessment. However, it was noted that the main factor affecting the assessment was the insertion depth. No association was found between the type of array and impact of image fusion (Fisher's exact test; $p = 0.956$). The presence of the significant impact of image fusion was associated with a deeper insertion of an electrode array, with the mean IDAs predicting a significant impact versus no impact being 452 and 392 degrees (t test; $p = 0.016$).

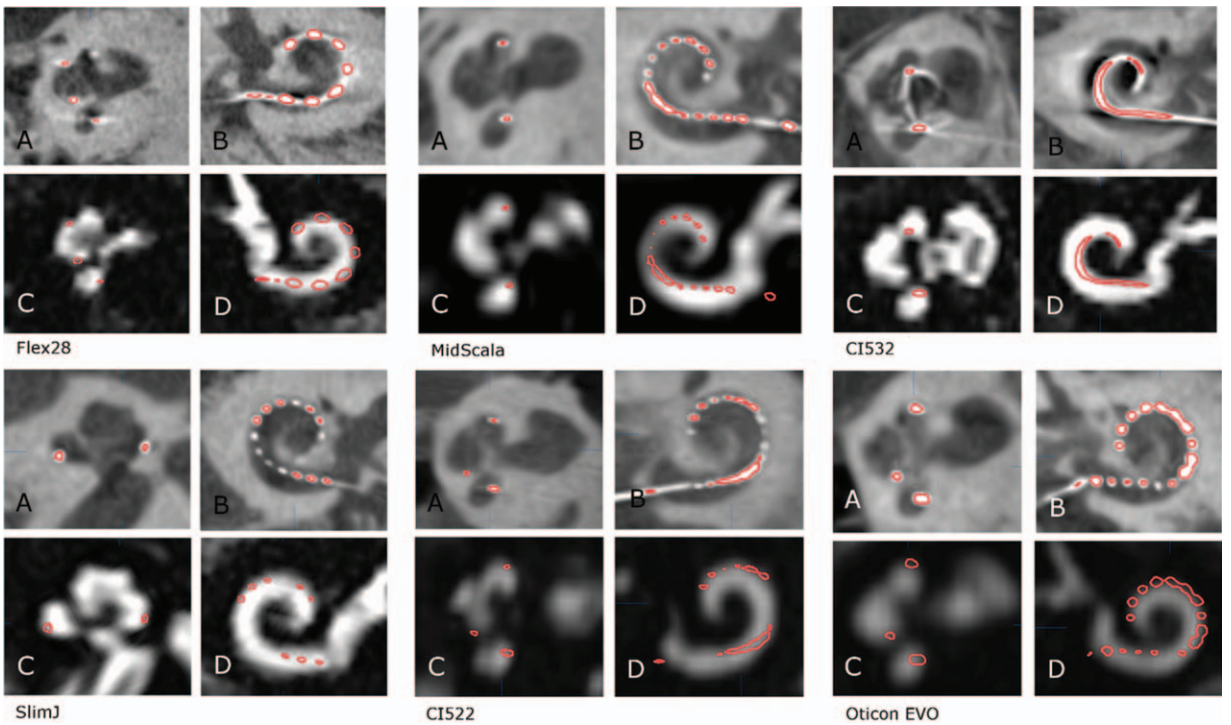

FIG. 1. The typical characteristics of each array on CBCT (*A–B*) and the HU segmented reconstruction (*red line*) on both CBCT and MRI (*C–D*). Med-El Flex28: Some artefact. Due to the extensive length of the array, the image fusion helps with apical evaluation, and in basal evaluation in some cases. Advanced Bionics, MidScala: Mostly symmetrical, round artefacts, which do not hinder the location assessment with CBCT. One case with many artefacts. Cochlear CI532: Many artefacts with bone-blurring halos, rays and arches. There is a mostly continuous artefact along the linear length. Image fusion helps considerably. Advanced Bionics SlimJ: Mostly round and symmetrical artefacts, some ray halos and tails. Image fusion helps in apical evaluation in some cases. Cochlear CI522: Symmetrical round artefacts, some lining up. Image fusion helps in some cases, mostly apically. Oticon EVO: Round moderate size artefacts that line up to some extent. Because of the deep insertion length, image fusion helps not only with the apical assessment but also with the basal evaluation. CBCT indicates cone-beam computed tomography; HU, Hounsfield unit; MRI, magnetic resonance imaging.

DISCUSSION

To the best of our knowledge, this is the first study, which has systematically evaluated the benefits of image fusion technique in postoperative cochlear implant imaging with different electrode arrays.

Although CBCT can be considered the method of choice for postoperative CI imaging, electrode artefacts reduce the image quality and impair the reliable assessment of the scalar placement and trauma. Güldner et al. (13) analyzed electrode artefacts with different CBCT imaging parameters in temporal bones and found no significant differences in artefact diameter for different voltages, currents, or exposure times. They concluded that the evaluation of the electrode both in the basal and the apical cochlea could not be improved by varying the scanning protocol.

Since the preoperative image data is readily available, we consider image fusion to be a beneficial supplement in ambiguous cases. Based on earlier studies, the fusion image technique was found to be a valid method for the reliable assessment of insertion trauma (18,20). With growing experience, it has become a semi-automatic and thus time-efficient procedure. The HRCT and CBCT fusions can be reconstructed automatically with only marginal manual input. Both HRCT and CBCT visualize in sharp detail the bony boundaries of the skull, hence the inner ear structures within the temporal bone are accurately fused by the automatic script. MRI and CBCT were fused semi-automatically requiring more manual assistance. All fusions were visually double-checked for accuracy by the authors. The advantages of MRI fusion are that it provides a clearer depiction of the apical topography than can be achieved with CT/CBCT, and it often identifies the BM. Therefore, MRI fusions acquire a more accurate evaluation than CT fusions. In two cases, however, the HRCT fusions were found to be more precise for determining the trauma grading.

Previous studies have reported that the exact assessment of the electrode location is often limited to the basal turn (13–15,24). One of the main findings of this study was that the benefits of image fusion increased in deeper insertions and towards the apex where the narrowing structures are easily blurred by artefacts. For insertions over 360 degrees, image fusions significantly improve the assessment of electrode placement and insertion trauma (Figs. 2 and 3). In addition, in cases in which profuse artefacts blur the cochlear structures, image

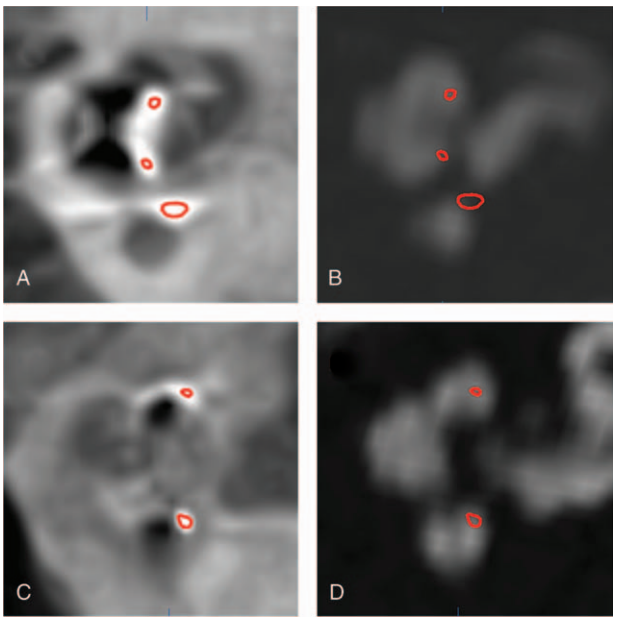

FIG. 2. Electrode reconstructions (red) of a CI532 (*A* and *B*), and of a Mid-Scala electrode (*C* and *D*). The postoperative CBCTs are illustrated on the left and MRI/CBCT fusions on the right. HU segmentation delineates the actual electrode within the artefact. Image fusion reconstructions allow for a more accurate evaluation of the electrode location with respect to the surrounding structures. CBCT indicates cone-beam computed tomography; MRI, magnetic resonance imaging.

fusion reconstructions make it possible to have a very precise assessment of the location of the electrode within the cochlea.

The Hounsfield unit (HU) is a quantitative measure describing the radiodensity of a substance in CT. It provides an accurate density for each substance and can be used for the identification of different types of tissue or substances in the region of interest. By applying HU segmentation, an electrode contact can be identified with better accuracy than by visual assessment alone, even if there are large artefacts present (Fig. 3).

At our institution postoperative CBCT scanning is performed with a device which allows the patient to sit with his/her head stabilized against a frame to minimize head movements. The imprecision caused by motion artefacts could be further minimized by utilizing supine devices. The intensity and pattern of the artefacts may appear different for other CBCT devices. Therefore, we chose not to quantify and compare the actual size of artefacts as we anticipated that they would be at least partly device-specific. The method described in this study can be generally applied also with different devices.

As we did not quantify the dimensions of the artefacts, we could not compare them with the properties of the arrays nor evaluate whether the fusion would be more helpful with increasing amounts of artefact.

The raw data of the preoperative CT imaging was no longer available for the image fusion, and therefore, we could not use the optimal resolution in the reconstructions. Better image quality and fusion reconstructions could be accomplished with thinner HRCT slices (0.6–0.4 mm).

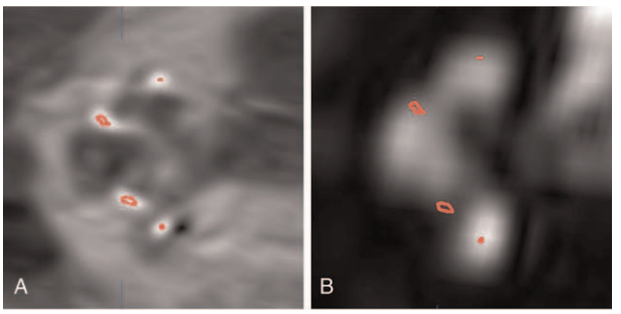

FIG. 3. Deep insertion (insertion depth angles [IDA] = 610 angles) with Flex28. The identification of the cochlear structures, especially after the basal turn, is deteriorated by the metallic artefacts on the postoperative CBCT (*A*). In the MRI image fusion reconstruction (*B*), the cochlear anatomy can be better depicted and hence the related electrode locations. CBCT indicates cone-beam computed tomography; MRI, magnetic resonance imaging.

We propose that postoperative radiological evaluation after cochlear implantation offers advantages in both clinical and research work. In the future, it might provide details to reveal a causal connection of insertion trauma and clinical outcomes, and could be helpful in the development of new arrays and surgical techniques. In the clinic, image fusions should be obtained in cases where CBCT alone is insufficient for evaluating insertion trauma.

CONCLUSION

By the application of an image fusion technique, a more accurate evaluation of electrode location was possible for all types of electrodes. Fusion images were especially helpful for the assessment of electrode location in deeper insertions (>360 degrees).

Acknowledgments: The authors would like to thank the Kuopio University Hospital (VTR), the Finnish Academy and the Pohjois-Savon maakuntarahasto for providing funding to help the Kuopio Cochlear Implant Research group to conduct this study, and acknowledge the assistance of Tuomas Selander in the statistical analysis.

REFERENCES

1. Holden LK, Finley CC, Firszt JB, et al. Factors affecting open-set word recognition in adults with cochlear implants. *Ear Hear* 2013;34:342–60.
2. Finley CC, Holden TA, Holden LK, et al. Role of electrode placement as a contributor to variability in cochlear implant outcomes. *Otol Neurotol* 2008;29:920–8.
3. O'Connell BP, Cakir A, Hunter JB, et al. Electrode location and angular insertion depth are predictors of audiologic outcomes in cochlear implantation. *Otol Neurotol* 2016;37:1016–23.
4. Nordfalk KF, Rasmussen K, Hopp E, Greisiger R, Jablonski GE. Scalar position in cochlear implant surgery and outcome in residual hearing and the vestibular system. *Int J Audiol* 2014;53:121–7.

5. O'Connell BP, Hunter JB, Wanna GB. The importance of electrode location in cochlear implantation. *Laryngoscope Investig Otolaryngol* 2016;1:169–74.
6. Dietz A, Wennström M, Lehtimäki A, Löppönen H, Valtonen H. Electrode migration after cochlear implant surgery: more common than expected? *Eur Arch Otorhinolaryngol* 2016;273:1411–8.
7. Aschendorff A. Imaging in cochlear implant patients. *GMS Curr Top Otorhinolaryngol Head Neck Surg* 2011;10:Doc07.
8. Alam-Eldeen MH, Rashad UM, Ali AHA. Radiological requirements for surgical planning in cochlear implant candidates. *Indian J Radiol Imaging* 2017;27:274–81.
9. Ruivo J, Mermuys K, Bacher K, Kuhweide R, Offeciers E, Casselman JW. Cone beam computed tomography, a low-dose imaging technique in the postoperative assessment of cochlear implantation. *Otol Neurotol* 2009;30:299–303.
10. Kennedy TA, Connell N, Szczykutowicz T, et al. Flat-panel CT for cochlear implant electrode imaging: comparison to multi-detector CT. *Otol Neurotol* 2016;37:1646–53.
11. Razafindranaly V, Truy E, Pialat J, et al. Cone beam CT versus multislice CT: radiologic diagnostic agreement in the postoperative assessment of cochlear implantation. *Otol Neurotol* 2016;37:1246–54.
12. Theunisse HJ, Joemai RMS, Maal TJJ, Geleijns J, Mylanus EAM, Verbist BM. Cone-beam CT versus multi-slice CT systems for postoperative imaging of cochlear implantation–a phantom study on image quality and radiation exposure using human temporal bones. *Otol Neurotol* 2015;36:592–9.
13. Güldner C, Wiegand S, Weiss R, et al. Artifacts of the electrode in cochlea implantation and limits in analysis of deep insertion in cone beam tomography (CBT). *Eur Arch Otorhinolaryngol* 2012;269:767–72.
14. De Seta D, Mancini P, Russo FY, et al. 3D curved multiplanar cone beam CT reconstruction for intracochlear position assessment of straight electrodes array. A temporal bone and clinical study. *Acta Otorhinolaryngol Ital* 2016;36:499–505.
15. Guldner C, Weiss R, Eivazi B, Bien S, Werner JA, Diogo I. Intracochlear electrode position: evaluation after deep insertion using cone beam computed tomography. *HNO* 2012;60:817–22.
16. Dees G, van Hoof M, Stokroos R. A proposed method for accurate 3D analysis of cochlear implant migration using fusion of cone beam CT. *Front Surg* 2016;3:2.
17. Dietz A, Iso-Mustajärvi M, Sipari S, Tervaniemi J, Gazibegovic D. Evaluation of a new slim lateral wall electrode for cochlear implantation: an imaging study in human temporal bones. *Eur Arch Otorhinolaryngol* 2018;275:1723–9.
18. Iso-Mustajärvi M, Matikka H, Risi F, et al. A new slim modiolar electrode array for cochlear implantation: a radiological and histological study. *Otol Neurotol* 2017;38:e334.
19. Sipari S, Iso-Mustajarvi M, Lopponen H, Dietz A. The insertion results of a mid-scala electrode assessed by MRI and CBCT image fusion. *Otol Neurotol* 2018;39:e1025.
20. Sipari S, Iso-Mustajarvi M, Matikka H, et al. Cochlear implantation with a novel long straight electrode: the insertion results evaluated by imaging and histology in human temporal bones. *Otol Neurotol* 2018;39:e793.
21. Jiang ZY, Odiase E, Isaacson B, Roland PS, Kutz JW. Utility of MRIs in adult cochlear implant evaluations. *Otol Neurotol* 2014;35:1533–5.
22. Connor SEJ. Contemporary imaging of auditory implants. *Clin Radiol* 2018;73:19–34.
23. Young JY, Ryan ME, Young NM. Preoperative imaging of sensorineural hearing loss in pediatric candidates for cochlear implantation. *Radiographics* 2014;34:E133–49.
24. Saeed SR, Selvadurai D, Beale T, et al. The use of cone-beam computed tomography to determine cochlear implant electrode position in human temporal bones. *Otol Neurotol* 2014;35:1338–44.